HHS Public Access

Author manuscript

Cancer Prev Res (Phila). Author manuscript; available in PMC 2019 May 01.

Published in final edited form as:

Cancer Prev Res (Phila). 2018 May ; 11(5): 265–278. doi:10.1158/1940-6207.CAPR-17-0349.

Pharmacological TLR4 antagonism using topical resatorvid blocks solar UV-induced skin tumorigenesis in SKH-1 mice

Karen Blohm-Mangone[1], **Nichole B. Burkett**[1], **Shekha Tahsin**[1], **Paul B. Myrdal**[3], **Alhassan Aodah**[3,4], **Brenda Ho**[1], **Jaroslav Janda**[1], **Michelle McComas**[1], **Kathylynn Saboda**[1], **Denise J. Roe**[1,5], **Zigang Dong**[6], **Ann M. Bode**[6], **Emanuel F. Petricoin III**[7], **Valerie S. Calvert**[7], **Clara Curiel-Lewandrowski**[1,8], **David S. Alberts**[1,8], **Georg T. Wondrak**[1,9], and **Sally E. Dickinson**[1,2,*]

[1]The University of Arizona Cancer Center, Tucson, Arizona

[2]Department of Pharmacology, The University of Arizona, Tucson, Arizona

[3]Department of Pharmacy Practice and Science, The University of Arizona, Tucson, Arizona

[4]The National Center for Pharmaceutical Technology, King Abdulaziz City for Science and Technology, Riyadh, Saudi Arabia

[5]Mel and Enid Zuckerman College of Public Health, The University of Arizona, Tucson, Arizona

[6]Department of Molecular Medicine and Biopharmaceutical Sciences, The Hormel Institute, The University of Minnesota, Austin, Minnesota

[7]Center for Applied Proteomics and Molecular Medicine, George Mason University, Manassas, Virginia

[8]Department of Medicine, The University of Arizona, Tucson, Arizona

[9]Department of Pharmacology and Toxicology, The University of Arizona, Tucson, Arizona

Abstract

An urgent need exists for the development of more efficacious molecular strategies targeting non-melanoma skin cancer (NMSC), the most common malignancy worldwide. Inflammatory signaling downstream of Toll-like receptor 4 (TLR4) has been implicated in several forms of tumorigenesis, yet its role in solar UV-induced skin carcinogenesis remains undefined. We have previously shown in keratinocyte cell culture and SKH-1 mouse epidermis that topical application of the specific TLR4 antagonist resatorvid (TAK-242) blocks acute UV-induced AP-1 and NF-κB signaling, associated with downregulation of inflammatory mediators and MAP Kinase phosphorylation. We therefore explored TLR4 as a novel target for chemoprevention of UV-induced NMSC. We selected the clinical TLR4 antagonist resatorvid based upon target specificity, potency, and physico-chemical properties. Here we confirm using *ex-vivo* permeability assays that topical resatorvid can be effectively delivered to skin, and using *in vivo* studies that topical resatorvid can block UV-induced AP-1 activation in mouse epidermis. We also report that in a UV-

*Corresponding author: Sally E. Dickinson, 1515 N. Campbell Ave., AZCC Rm. 3977, Tucson, AZ 85724, phone: 520-626-8208, fax: 520-626-4979, sdickinson@uacc.arizona.edu.

The authors declare no potential conflicts of interest.

induced skin tumorigenesis model, topical resatorvid displays potent photochemopreventive activity, significantly suppressing tumor area and multiplicity. Tumors harvested from resatorvid-treated mice display reduced activity of UV-associated signaling pathways and a corresponding increase in apoptosis compared to tumors from control animals. Further mechanistic insight on resatorvid-based photochemoprevention was obtained from unsupervised hierarchical clustering analysis of protein readouts via reverse-phase protein microarray revealing a significant attenuation of key UV-induced proteomic changes by resatorvid in chronically treated high-risk SKH-1 skin prior to tumorigenesis. Taken together, our data identify TLR4 as a novel molecular target for topical photochemoprevention of NMSC.

Keywords

TLR4; photochemoprevention; resatorvid; SKH-1; NMSC

Introduction

Toll-like receptors (TLRs) are transmembrane proteins responsible for detecting diverse pathological stimuli and alerting the innate immune system for host defense. There are 11 isoforms of TLRs found in humans, many of which have attracted attention due to their roles in acute and chronic diseases. One isoform, TLR4, is overexpressed in many forms of cancer (1). The canonical ligand for TLR4 is the glycolipid lipopolysaccharide (LPS) derived from gram-negative bacteria (2). However, TLR4 dimerization and downstream signal transduction can also be stimulated by other pathogen-associated molecular patterns (PAMPs), such as certain viral proteins and cleaved fibrinogen, and damage-associated molecular patterns (DAMPs), such as HMGB1, HSP70 and oxidized LDL (reviewed in (3)). TLR4 has now been identified as a novel molecular target for clinical interventions directed at pathologies including septic shock, diabetes, asthma and cancer (4–7).

Non-melanoma skin cancer (NMSC) affects 5 million people in the US each year and is directly linked to cutaneous exposure to ultraviolet (UV) rays from the sun (8–10). UV exposure leads to DNA damage, oxidative stress and, over time, dysregulation of cellular signaling (11). Proper immune surveillance of damaged cells in the skin is crucial for the repression of skin cancer, as people undergoing chronic immune suppression are at a 60-100 fold increased risk of developing NMSC compared to the general population (12). However, overstimulation of inflammation also plays a major causative role in skin carcinogenesis (13, 14), and reducing aberrant inflammation of the skin is required to prevent stimuli associated with tumor progression. Blocking inflammatory pathways using genetic or pharmacological means can prevent UV-induced skin cancer in mice (15–17), and long-term non-steroidal anti-inflammatory drug use is associated with reduced risk of NMSC in humans (18).

TLR4 has now been identified as a major driver of cutaneous inflammation (19). In addition to expression in immune cells, TLR4 is expressed in keratinocytes, allowing stimulation from endogenous ligands (e.g. HMGB1) released from other cells in response to cytotoxic environmental stress including UV (20, 21). Ligand-induced TLR4 activation orchestrates cutaneous inflammatory signaling through downstream effectors including myeloid

differentiation factor 88 (MyD88), Akt (PKB), activator protein-1 (AP-1), and nuclear factor κB (NF-κB) (22, 23). Importantly, TLR4 overexpression is an emerging hallmark of NMSC and melanoma, and a crucial role of TLR4 in chemically-induced inflammatory carcinogenesis has been demonstrated in murine skin (19, 21). However, the contribution of keratinocyte-derived TLR4 activity in response to UV and its connection to photocarcinogenesis has not been well characterized.

Recently, we have shown that TLR4 activity contributes to the stimulation of cell stress responses after treatment of keratinocytes with UV upstream of NF-κB, AP-1 and Akt, all of which are established targets for molecular photochemoprevention (24–27). In addition, we observed that the thickness of the layer of TLR4-expressing keratinocytes increases during the progression from normal human skin (only the basal layer of keratinocytes) to actinic keratoses (AK) to squamous cell carcinoma (SCC). Using a targeted small molecule inhibitor of TLR4 cytoplasmic activity (resatorvid; TAK-242, CAS No. : 243984-11-4, Fig. 1A), we showed that treatment of keratinocytes in culture as well as topical treatment of mouse skin prevents UV-induced MAPkinase and NF-κB stimulation, together with potentiation of acute UV-induced epidermal apoptosis (24). Takashima et al. (2009) used mutational analysis and radiolabeled resatorvid to demonstrate TLR4 specificity through irreversible adduction of a specific intracellular domain cysteine residue (Cys747, (28)). This adduction disrupts TLR4 TIR-domain interaction with its downstream adaptor molecules (including MyD88 and TRAM/TRIF (28, 29)), thereby causing sustained suppression of TLR4-dependent signaling. Resatorvid has displayed an excellent safety profile in systemic clinical trials and does not absorb in the relevant solar UV spectrum (24, 30). Therefore, based upon our prior observations, we decided to investigate the potential photochemopreventive effects of resatorvid-based TLR4 antagonism in skin. Our data presented in this study demonstrate that topical TLR4 inhibition effectively blocks UV-induced skin stress signaling and tumorigenesis in SKH-1 hairless mice with no observable toxicity, providing critical evidence in support of ongoing efforts towards clinical testing of topical resatorvid formulations on human skin.

Materials and Methods

Materials

Resatorvid (TAK-242) was purchased from MedChem Express (Monmouth Junction, NJ). Most antibodies were purchased from Cell Signaling Technology (Danvers, MA) including phospho-p38 (9215), total p38 (8690), phospho-Akt (4060), $p21^{waf1}$ (2946), cleaved caspase 3 (9661) and beta tubulin (5666). The beta actin antibody was purchased from Sigma-Aldrich (A5441, St. Louis, MO), and the TLR4 antibody was purchased from Santa Cruz Biotechnology (sc-293072, Dallas, TX). The Ki67 antibody (Supplemental Fig. 1) was purchased from Leica Biosystems (ACK02, Buffalo Grove, IL).

Cutaneous pharmacokinetics study using the Franz cell permeation chamber—The standard use of Franz cell permeation chamber systems to assess skin pharmacokinetics of drugs in topical and transdermal drug delivery systems has been published extensively (31, 32). Briefly, murine SKH-1 skin was harvested and the

underlying adipose tissue was removed. Each skin segment was inserted between the receiver and donor chambers of the cell, with the stratum corneum facing upwards, as reported elsewhere (31). Following our previous *in vivo* murine experimentation protocol, resatorvid (13 mM in acetone; 66 μL) was applied to the top of nine Franz diffusion cells (Skin Penetration System 3, Laboratory Glass Apparatus, Berkeley, CA; Franz cell contact surface area: 0.9 cm^2, n = 3) (24). The receiver cell was filled with 4 mL of circulating PBS (pH 7.4). The experiments were conducted at 32 °C and monitored over 8 hours.

Franz cells were disassembled at various time points, and each skin segment was subjected to 3 rounds of tape stripping of the non-viable stratum corneum. Tape strips 4-12 were also collected for epidermal removal and analyzed separately. The remaining dermal skin layer was diced and sonicated in isopropyl alcohol for 10 minutes using a probe sonicator, followed by centrifugation (1400 rpm, RT). After supernatant filtration, quantitative HPLC analysis was performed. For quantification of total cutaneous resatorvid delivery (after removal of stratum corneum from live skin), epidermal and dermal drug contents were analyzed separately and combined (Fig. 1A).

HPLC analysis—A reverse-phase HPLC system using a Waters 2690 separation module coupled with a Waters 2487 Dual wavelength detector (254 nm), and a Symmetry C18 5 μm column (150 mm × 2.1 mm, maintained at 25 ± 2°C; Waters, Milford, MA, USA), was used. Mobile phase conditions were 40:60 (v/v) ACN: Trifluoroacetic acid (0.1% v/v) at a flow rate of 0.3 ml/min. Quantification was performed using peak area and calculated from a five-point standard curve.

Photo-stability of resatorvid—Photo-stability was examined by preparing two sets of samples (80.6 μg/ml of resatorvid in 100% acetone or 4.9 μg/ml of resatorvid in water), each containing three samples including a control. Each sample was prepared in a transparent HPLC glass vial and closed without any entrapped air. Solar simulated light (SSL) exposure was performed using UVA340 lightbulbs (Q-lab Corporation) with emission between 295 and 390 nm (50 kJ UVA/m^2 and 2.4 kJ UVB/m^2; dose 1×) whereas controls remained unexposed (25). Additional samples were exposed to a double dose of SSL (dose 2×). After exposure, resatorvid content was analyzed using HPLC. It should also be noted that separate experimentation showed that resatorvid displays no significant absorption in the relevant solar UV spectrum (24).

Chemical stability of resatorvid solutions at ambient temperature—Resatorvid solutions were prepared in several different media: acetone, citrate buffer (pH 3), phosphate buffer (pH 5.2 and 7.4), and borate buffer (pH 9). Each solution was stored in glass vials at ambient temperature (25 °C). A sample was withdrawn 9, 37 and 64 days post preparation, and drug concentration was measured by HPLC.

Mouse epidermal luciferase assay—Age and sex-matched SKH-1 mice expressing the TRE-luciferase reporter gene (AP-1 luciferase mice, bred in-house) were utilized for this study, as reported previously (n = 14 for acetone, n = 9 for resatorvid) (26, 33). The ears of the mice were treated twice with resatorvid prior to acute UV exposure: 24hr prior and 1hr prior (10mM resatorvid in acetone, 50 μL/ear). To induce AP-1 signaling in the skin, mice

were then exposed to 2.75 kJ/m^2 UVB, and three 3 mm ear punches were collected from the right ear after sacrifice 48 hr later. An additional three 3 mm punches were collected from the left ear of each mouse after 24 hr/1 hr resatorvid exposure but 24 hr prior to UV as an internal control. All ear punches were processed for luciferase assay as described previously (27). All mice were housed and treated in accordance with The University of Arizona Animal Care and Use Committee standards under an approved protocol (#08-153).

Reverse-Phase Protein Microarray (RPPA) of high-risk mouse skin—Epidermal protein lysates were generated from four groups of female SKH-1 mice (SKH1-*Hr*^{hr}, Charles River laboratories) exposed to a chronic UV treatment regimen to generate tumor-prone high-risk skin according to standard protocols in parallel with other mice used for the tumorigenesis study, described below (25, 34). These groups consisted of chronic solar UV + topical vehicle (acetone), chronic UV + topical resatorvid, no UV + topical vehicle, or no UV + topical resatorvid. For all groups, vehicle or resatorvid was applied to the back in a designated area, three times a week, 1 hr prior to each UV exposure (or without UV for control groups). All groups were sacrificed 24hr after their last UV exposure on week 14. This chronic exposure is sufficient to induce a significantly damaged epidermis without visible signs of tumors, which start to emerge 1-2 weeks later. Snap frozen epidermis was scraped from the dermis and ground to a powder using a frozen mortar and pestle. Samples from each skin were subjected to lysis and protein pathway activation mapping using RPPA under established protocols (25). Unsupervised two-way hierarchical clustering (JMP, SAS Institute, Inc.) was used to generate a heatmap, where red indicates a higher relative expression of a protein/phosphoprotein and green indicates a lower relative expression of a protein/phosphoprotein. Black indicates no relative change within the population analyzed.

High-risk SKH-1 mouse skin and photocarcinogenesis study—Female SKH-1 mice were utilized for analysis of the effect of resatorvid on skin tumorigenesis. Six to eight-week old mice were exposed to solar-simulated light (solar UV) using a bank of 6 UVA340 bulbs (Q-lab Corporation) as described previously (25). Briefly, mice were divided into three groups (n = 20): Acetone (vehicle), Resatorvid Prevention (or “early prevention”), and Resatorvid Intervention (or, “late prevention”). All mice were exposed to UV three times a week for 15 weeks exactly as before (25). One hour prior to each UV exposure, mice were treated topically with either 200 μL of acetone on their backs (acetone and intervention groups), or with 200 μL of 10 mM resatorvid (prevention group). After week 15, all UV treatments stopped, but Acetone and Prevention groups continued to receive the same topical treatments three times a week. The Intervention group switched from acetone to resatorvid topical treatments three times a week after week 15 (Fig. 2A). Mice were harvested at week 25, 24hr after their last treatment. The chronically exposed “dropout” (high-risk) mice described above were treated alongside this tumor study, but harvested at week 14 as described. After sacrifice at week 25, tumors were harvested from each group and either snap frozen or formalin fixed for paraffin embedding. Whenever possible, large cutaneous SCCs (cSCCs) were split and both fixed and frozen.

Western blots—Frozen cutaneous SCCs from the above tumorigenesis study and frozen epidermis scraped from the dropout mice were ground to powder using a frozen mortar and

pestle and used for Western blot analysis as previously described (25, 35). Membranes were typically split to probe for multiple proteins, and only stripped and re-probed for loading controls. All blots were performed at least twice to confirm results. Densitometry of bands was performed using Image J (NIH).

Immunohistochemistry and Tissue Staining—Staining of mouse SCCs for cleaved caspase 3 and Ki67 was performed on FFPE slides according to protocols slightly modified from those described previously (27). Slides were then counterstained with 25% Hematoxylin Gill III (Leica Biosystems [Surgipath], Germany). Immunohistochemical staining of tumors from the Acetone group (n = 6), Intervention and Prevention groups (n = 4 each) was quantified using ImagePro Plus software (Media Cybernetics), a Leica DMR microscope, and a Sony 3CCD color video camera. The mean positive cellular area per 40× field was determined by averaging the measurements of three representative fields in each tumor. H&E-based quantification of epidermal immune cell infiltrates classified as "lymphocytic" according to standard morphological criteria (agranular leukocytes containing small, round nuclei and minimal cytoplasm) was performed by a board-certified pathologist.

Statistical analysis—The mouse luciferase experiments were analyzed by computing the fold induction reading for each mouse, by dividing the individual post-UV luciferase readings by the matched pre-UV luciferase readings. The fold changes were converted to Log_{10} format for graphing. A Wilcoxon Rank Sum Test was used (on the raw data) to statistically compare the two groups (acetone versus resatorvid treated). For other comparisons, two sample independent *t* tests were used to compare two groups, and ANOVA with Bonferroni post-hoc adjustment for was used to compare three or more groups. Means, standard deviations and other summary statistics were calculated by treatment group for tumor volume and tumor count. The Kaplan-Meier method was used to estimate tumor latency; comparisons between groups were performed using a log-rank test. Univariate cross sectional analyses compared tumor count and tumor volume at 25 weeks of observation by treatment groups using the Kruskal Wallis Test. All pairwise comparisons were made using the Wilcoxon Rank Sum test. Alpha levels were set at 0.05. For post hoc multiple comparisons alpha was Bonferroni corrected and set at p=0.0167. For all figures, the '*' indicates a p value at or lower than the cutoff for statistical significance. After log transformations to achieve approximate normality, multivariate analysis compared tumor count and tumor volume across the weeks of observation by treatment using mixed effects models. This accounted for the correlations between the measurements obtained across days for the individual mice (slope analysis). All analyses were conducted using STATA 14.

Results

Topical resatorvid achieves extended mouse skin residence time with minimal transdermal delivery

Dorsal skin from SKH-1 hairless mice was excised and used to examine the transdermal penetration properties of topical resatorvid. The concentration of resatorvid (13 mM) and the diluent (acetone) replicate the solution we have used previously to successfully modulate

UV-induced biomarkers in SKH-1 skin (24). Using a standardized Franz cell system, examination of the living layers of the skin (epidermis, dermis), and receiver fluid over a timecourse using HPLC reveals that resatorvid efficiently penetrates the stratum corneum and remains in the skin for a period of at least 8 hr, at which time it reaches a concentration of 47 μg/cm^2 (Fig. 1A). There is minimal transdermal penetration of the agent until after four hours, where it reaches a flux of 10 μg/cm^2 (Fig. 1A). While a significant amount of agent remained in the stratum corneum (tape strips 1-3), the amount of resatorvid in the lower epidermis (tape strips 4-12) was constant throughout the timecourse at an average of 5 μg/cm^2 (Fig. 1A, dark grey bars). Thus, the average resatorvid transdermal flux was calculated to be 2.50 ± 0.08 (μg/cm^2/hr) with a lag time 4.50 ±0.12 hours. However, the average flux to the dermis was 4.4 ± 1.34 (μg/cm^2/hr) with a lag time of less than 1 hr.

Resatorvid exhibits good stability in organic solution

The stability of resatorvid under conditions of UV exposure and differing pH was examined. Resatorvid in water, when exposed to UV degraded more readily than when the compound was dissolved in acetone (Fig 1B). When the compound was exposed to solutions of varying pH over time, resatorvid displayed minimal degradation during 64 days at room temperature in acetone and aqueous solution (pH 3 to 7.4), maintaining at least 90% of the original concentration over time. However, significant degradation of the compound occurred at pH 9, dropping to 51.3% remaining at day 64 (Fig. 1C).

Resatorvid inhibits UV-induced AP-1 signaling in mouse epidermis

In order to test the efficacy of topical resatorvid administration on UV-induced skin inflammatory signaling, transgenic SKH-1 AP-1 luciferase reporter mice were employed as described previously (26, 27). Analysis of the raw data revealed inhibition of UVB-induced AP-1 transcriptional activation as a result of topical resatorvid treatment, an effect approaching statistical significance ($p = 0.05$, Fig. 1D). These data are consistent with our previous observation that topical resatorvid suppresses UV-induced inflammatory markers (NF-κB, p38) as quantified by Western blot analyses in SKH-1 mouse skin (Fig. 1E, F) (24).

Topical TLR4 antagonism using resatorvid attenuates chronic UV-induced stress responses in the epidermis of high risk SKH-1 mice

Next, we examined the effects of resatorvid treatment in a model of chronic UV exposure. SKH-1 hairless mice were therefore exposed to topical acetone (200 μL/back) +/− UV or 200 μL of 10 mM resatorvid in acetone +/− UV three times a week for 14 weeks and were sacrificed as controls for an ongoing tumorigenesis experiment (Fig. 2A). These high-risk mice had no visible tumors at the time of harvest, and treatment with acetone or resatorvid did not cause noticeable toxicity or inflammation of the skin. H&E-based quantification by a board-certified pathologist indicate that resatorvid efficiently blocked UV-induced epidermal immune cell infiltration, identified as primarily lymphocytic based on standard morphological characteristics (Fig. 2B, $p < 0.001$). Epidermal lysates from each mouse ($n = 5$ for No UV groups, $n = 4$ for +UV groups) were subjected to comprehensive protein pathway activation mapping using RPPA to quantitate protein expression levels and phosphorylation status under established protocols (25, 36). Unsupervised two-way hierarchical clustering was used to generate a heatmap of the resulting data, which notably

resulted in each group clustering together in a predictable array: acetone No UV, resatorvid No UV, acetone + UV and resatorvid + UV (Fig. 2C).

This expression clustering by treatment group was also observable at the level of individual UV-modulated proteins. For example, in a large cluster of analytes, resatorvid treatment consistently antagonized UV-induced changes, such as activation of the transcription factor Stat3 (Y705), the Akt regulatory protein PDK1 (S241), the inflammatory cytokine IL-6 and total levels of p62/SQSTM1, a ubiquitin binding protein which has been implicated in the regulation of NF-kB and autophagy (37–39) (Fig. 2D). Consistent with suppression of stress response signaling by chronic UV exposure, resatorvid treatment attenuated phosphorylational activation of NFκB (p65 S536) and p53 (S15) (Fig. 2E, middle and right panel), as well as cleaved PARP, Stat1 (Y701), Stat5 (Y694), PAK1/2 (T423/402), and Chk-2 (S33/35) (Fig. 2E left panel). Together, results from these chronically UV-exposed high-risk epidermal samples indicate that topical resatorvid treatment dramatically antagonizes UV-induced expression changes of multiple proteins involved in stress signaling, inflammation and apoptosis.

Topical TLR4 antagonism using resatorvid significantly reduces UV-induced skin tumorigenesis in SKH-1 mice

In order to establish the photochemopreventive efficacy of resatorvid-based TLR4 antagonism, two treatment regimens were implemented in female SKH-1 hairless mice. For the Prevention group, resatorvid was used in conjunction with UV, while for the Intervention group, resatorvid administration was implemented after chronic UV treatments had stopped, as detailed in the Methods section (Fig. 2A). Tumor volume and multiplicity were monitored until sacrifice at week 25. Weekly weight measurements indicate that topical resatorvid treatment did not affect the average group weight gain over time, consistent with the absence of toxic effects at our dosage level (Fig. 3A). Strikingly, Kaplan-Meier survival modeling reveals that mice on the Prevention protocol had a significantly increased tumor latency compared to acetone controls ($p < 0.001$), while mice on the Intervention protocol had an intermediate latency that was not significantly different from the other groups (Fig. 3B). At week 25, all surviving animals in the acetone control group had at least one tumor, while 15% and 45% remained tumor-free in the Intervention and Prevention groups, respectively (Fig. 3B).

This trend also held true for tumor burden (average tumor area per mouse) and tumor multiplicity (average tumors per mouse). In the case of tumor burden, at week 25 mice in the Prevention arm presented an average tumor area of 16.6 mm^2, the Intervention arm averaged 30.2 mm^2, and the Acetone control arm averaged 55 mm^2 ($p = 0.0077$ Prevention versus Acetone; Intervention not significantly different from other groups). (Fig. 3C). Furthermore, the tumor multiplicity at the end of the study also resulted in significant reductions of tumor counts in the Prevention arm (1.9 tumors/mouse) compared to the Acetone arm (3.8 tumors/mouse; $p = 0.037$), while the Intervention arm had intermediate numbers (2.55 tumors/mouse; not significantly different from the other groups) (Fig. 3D). Notably, multivariate mixed models regression analysis of the slopes across time of the Prevention and Intervention arms showed a statistically significant decrease in both tumor burden and

multiplicity slopes over weeks 14 – 26 compared to the acetone control ($p < 0.0001$ in all cases). The same analysis also showed that the slopes of the Prevention arm and Intervention arm were significantly different from each other for tumor multiplicity ($p < 0.001$) (Fig. 3C and 3D).

Topical TLR4 antagonism using resatorvid attenuates expression of UV-induced cell stress biomarkers and activates caspase 3 in SKH-1 mouse skin tumors

Snap frozen cSCC tumors collected at the end of the 25-week tumorigenesis study were subjected to Western blot analysis for markers of UV-induced skin stress responses. TLR4 protein expression was detected in every tumor tested. However, downstream signaling pathway activity between groups was markedly different. Phosphorylation of both Akt and p38 MAP Kinase were significantly reduced in tumors from the Prevention arm of the study compared to those from the Acetone arm ($p = 0.019$ and 0.005 for p-Akt and p-p38, respectively), while expression of total p38 remained fairly constant (Fig. 4A, quantified in Fig. 4B, C). There was also a remarkable reduction in average levels of $p21^{waf1}$ expression in the Prevention tumors compared to controls (Fig. 4A, quantified in Fig. 4D, $p = 0.047$). In contrast, even though similar trends were observed in response to the Intervention regimen, none of these expression changes (p-p38, p-Akt, p21) reached the level of statistical significance.

After obtaining this tumor tissue data, we also performed western blot analysis of the epidermal samples from high-risk (14 week dropout) mice used for RPPA (Fig. 3) to monitor whether these resatorvid-induced changes can occur at earlier stages of skin exposure to UV/drug (Fig. 4E). Notably, our analysis reveals that chronic treatment with UV caused a dramatic increase in the expression of TLR4 ($p = 0.0012$), an effect significantly antagonized by resatorvid treatment ($p = 0.016$) (Fig. 4F). In addition, chronic treatment with UV + acetone showed an expected increase in phosphorylation of p38 MAP Kinase and Akt (Ser473) compared to No UV controls (25, 40). However, UV-induced phosphorylation of p38 and Akt was further enhanced in the UV + resatorvid samples, in contrast to the compound's effects on TLR4 expression (Fig. 4E).

In addition, immunohistochemical (IHC) analysis from fixed samples taken from the same tumors indicated a significant impact of resatorvid treatment on survival signaling. Specifically, expression of the apoptotic marker cleaved caspase-3 was increased significantly in tumors from the Prevention group compared to those from the acetone control group (Fig. 4G, H; $p = 0.031$). Likewise, expression of the proliferation marker Ki67 was attenuated in these tumors by resatorvid treatment in the Prevention group compared to acetone controls; however, this trend did not reach the level of statistical significance (Supplemental Fig. 1).

Discussion

TLR4-directed molecular strategies targeting cancer have recently attracted considerable attention ((41, 42), reviewed in (1) and (19)). Here we present a first-in-kind study showing that topical resatorvid achieves significant skin residence time (Fig. 1A), attenuates UV-

induced AP-1 activation (Fig. 1D), and blocks photocarcinogenesis in mice (Fig. 3), an effect achieved without cutaneous or systemic resatorvid toxicity.

In the tumorigenesis model, co-treatment with resatorvid throughout the duration of the experiment (Prevention arm), resulted in a delayed onset of tumors in addition to significantly reduced burden and multiplicity compared to acetone-treated controls (Fig. 3). Furthermore, Western blot analysis of tumors harvested at the end of the study provide evidence that while TLR4 expression was maintained in all treatment groups, downstream stress signaling, i.e., UV-induced p-p38 and p-Akt, were significantly inhibited in the presence of resatorvid. Resatorvid treated tumors also displayed dramatically reduced expression of $p21^{waf1}$, which has been shown to block UV-induced apoptosis in keratinocytes (43). In addition, the Prevention group tumors demonstrated significantly higher levels of cleaved caspase-3 staining compared to the control group as observed previously in response to acute UV exposure (Fig. 4G, H) (24). These changes are consistent with resatorvid-induced alterations of survival signaling and a dramatic potentiation of epidermal apoptosis, which may underlie the chemopreventive activity of this agent (Fig. 5).

Importantly, initiation of resatorvid treatment after chronic UV exposure (Intervention arm) also reduced tumor burden and multiplicity, although this effect did not reach the level of statistical significance (Fig. 3C, D). However, slope analysis of the data over time indicates that both treatment regimens significantly affected the rates of tumor growth. It is tempting to speculate that the decreased sensitivity of high-risk mouse skin to resatorvid-based intervention is potentially due to alterations in cutaneous apoptotic response and DNA repair. As detailed above, we have now observed that in cell culture, in acute *in vivo* studies, and in tumors (Fig. 4G, H; (24)), resatorvid treatment when used concurrently with UV causes potentiation of apoptosis. In addition, the suppressive role of TLR4 on DNA repair has now been recognized (44). Therefore, even though TLR4 expression was increased in high-risk skin (Fig. 4E, F), pharmacological TLR4 antagonism initiated only at a late stage may be insufficient to block tumorigenesis after significant UV-induced DNA damage has already occurred.

Unsupervised hierarchical clustering analysis of protein readouts employing RPPA revealed a consistent attenuation of UV-induced proteomic changes by resatorvid in the epidermis prior to tumorigenesis. Almost one third of the >150 proteins analyzed displayed an expression pattern consistent with resatorvid suppression of UV-induced changes (Fig. 2C, E), affecting the expression of multiple proteins involved in stress signaling, inflammation and apoptosis (Fig. 2). These data demonstrate that resatorvid-dependent pathway modulation can be detected in high-risk mouse epidermis, indicative of early molecular markers of photochemoprevention.

Strikingly, Western blot analysis indicated that TLR4 protein expression was dramatically upregulated by long-term UV exposure, an outcome which was significantly inhibited by topical resatorvid treatment. As TLR4 protein expression is also significantly upregulated in human epidermis during the progression from normal skin to AK and cSCC, we feel that our high-risk mouse epidermal samples therefore represent a valid model for pre-tumorigenic human skin (24). The fact that resatorvid treatment reduced TLR4 upregulation in these

samples also suggests that this compound may be a promising chemopreventive agent for patients at high risk of cSCC.

Remarkably, p-p38 and p-Akt levels were higher in resatorvid-treated high-risk skins compared to their acetone treated controls, which contrasts with what was observed in the tumor Western blots for the same proteins. This may be due to changes in regulatory factors, such as the expression of microRNAs or protein phosphatases, which are known to be regulated by UV exposure but have not been examined in the context of chronic TLR4 inhibition in living epidermis (45, 46). We are continuing to examine the implications of resatorvid-induced regulation of these and other biomarkers in our ongoing studies.

Toll-like receptors have lately become promising molecular targets for clinical intervention in various human pathologies (4–7). Indeed, Imiquimod-based TLR7 agonism has become an approved treatment option for actinic keratosis and superficial basal cell carcinoma (47). Likewise, clinical studies have examined adjuvant use of TLR4 agonists combined with vaccines to enhance responses to microbial pathogens and tumor antigens (48). On the other hand, illustrating the complexity of TLR4-dependent pro- and anti-tumor responses, a causative role of TLR4 in chemotherapy-driven metastasis has been substantiated in paclitaxel-treated breast cancer patients (reviewed in (49)). Importantly, while it has recently been suggested that TLR4 may inhibit keratinocyte proliferation (50), solid published evidence strongly implicates TLR4 overexpression in NMSC and melanoma (1, 21, 24), and our own research has demonstrated that pharmacological TLR4 antagonism suppresses solar UV-induced inflammatory signaling (19, 24). Taken together, our findings for the first time demonstrate photochemopreventive efficacy of topical resatorvid, providing a rationale for further translational exploration of TLR4-directed antagonism targeting skin cancer in susceptible patient populations. Topical agents such as resatorvid may therefore be beneficial when used in combination with sunscreens to reduce inflammatory signaling and allow for clearance of UV-damaged cells in skin.

Supplementary Material

Refer to Web version on PubMed Central for supplementary material.

Acknowledgments

The authors wish to acknowledge the contributions of Mary Krutzsch, Michael Yoswiak and Dr. Agnes Witkiewicz.

Financial Support: All data was generated with the support of the following NIH grants: NCI P01 CA027502, Cancer Center Support Grant P30 CA023074 using the Tissue Acquisition and Cellular/Molecular Analysis Shared Resource, R03 CA212719, and pilot funding from the University of Arizona Skin Cancer Institute (SCI).

References Cited

1. Mai CW, Kang YB, Pichika MR. Should a Toll-like receptor 4 (TLR-4) agonist or antagonist be designed to treat cancer? TLR-4: its expression and effects in the ten most common cancers. Onco Targets Ther. 2013; 6:1573–87. Epub 2013/11/16. DOI: 10.2147/OTT.S50838 [PubMed: 24235843]
2. Gioannini TL, Teghanemt A, Zhang D, Levis EN, Weiss JP. Monomeric endotoxin:protein complexes are essential for TLR4-dependent cell activation. J Endotoxin Res. 2005; 11(2):117–23. Epub 2005/06/14. DOI: 10.1179/096805105X35198 [PubMed: 15949139]

3. Brubaker SW, Bonham KS, Zanoni I, Kagan JC. Innate immune pattern recognition: a cell biological perspective. Annu Rev Immunol. 2015; 33:257–90. Epub 2015/01/13. DOI: 10.1146/annurev-immunol-032414-112240 [PubMed: 25581309]
4. Awasthi S. Toll-like receptor-4 modulation for cancer immunotherapy. Front Immunol. 2014; 5:328. Epub 2014/08/15. doi: 10.3389/fimmu.2014.00328 [PubMed: 25120541]
5. Huang NQ, Jin H, Zhou SY, Shi JS, Jin F. TLR4 is a link between diabetes and Alzheimer's disease. Behav Brain Res. 2017; 316:234–44. Epub 2016/09/07. DOI: 10.1016/j.bbr.2016.08.047 [PubMed: 27591966]
6. Chattopadhyay S, Veleeparambil M, Poddar D, Abdulkhalek S, Bandyopadhyay SK, Fensterl V, et al. EGFR kinase activity is required for TLR4 signaling and the septic shock response. EMBO Rep. 2015; 16(11):1535–47. Epub 2015/09/06. DOI: 10.15252/embr.201540337 [PubMed: 26341626]
7. Fageras Bottcher M, Hmani-Aifa M, Lindstrom A, Jenmalm MC, Mai XM, Nilsson L, et al. A TLR4 polymorphism is associated with asthma and reduced lipopolysaccharide-induced interleukin-12(p70) responses in Swedish children. J Allergy Clin Immunol. 2004; 114(3):561–7. Epub 2004/09/10. DOI: 10.1016/j.jaci.2004.04.050 [PubMed: 15356557]
8. Guy GP Jr, Machlin SR, Ekwueme DU, Yabroff KR. Prevalence and costs of skin cancer treatment in the u.s., 2002-2006 and 2007-2011. Am J Prev Med. 2015; 48(2):183–7. Epub 2014/12/03. DOI: 10.1016/j.amepre.2014.08.036 [PubMed: 25442229]
9. Cadet J, Mouret S, Ravanat JL, Douki T. Photoinduced damage to cellular DNA: direct and photosensitized reactions. Photochem Photobiol. 2012; 88(5):1048–65. Epub 2012/07/12. DOI: 10.1111/j.1751-1097.2012.01200.x [PubMed: 22780837]
10. Clydesdale GJ, Dandie GW, Muller HK. Ultraviolet light induced injury: immunological and inflammatory effects. Immunol Cell Biol. 2001; 79(6):547–68. Epub 2002/03/21. DOI: 10.1046/j.1440-1711.2001.01047.x [PubMed: 11903614]
11. Bowden GT. Prevention of non-melanoma skin cancer by targeting ultraviolet-B-light signalling. Nat Rev Cancer. 2004; 4(1):23–35. [PubMed: 14681688]
12. Chockalingam R, Downing C, Tyring SK. Cutaneous Squamous Cell Carcinomas in Organ Transplant Recipients. J Clin Med. 2015; 4(6):1229–39. Epub 2015/08/05. DOI: 10.3390/jcm4061229 [PubMed: 26239556]
13. Lewis W, Simanyi E, Li H, Thompson CA, Nasti TH, Jaleel T, et al. Regulation of ultraviolet radiation induced cutaneous photoimmunosuppression by toll-like receptor-4. Arch Biochem Biophys. 2011; 508(2):171–7. Epub 2011/01/18. DOI: 10.1016/j.abb.2011.01.005 [PubMed: 21236239]
14. Hensler S, Mueller MM. Inflammation and skin cancer: old pals telling new stories. Cancer J. 2013; 19(6):517–24. Epub 2013/11/26. DOI: 10.1097/PPO.0000000000000010 [PubMed: 24270351]
15. Fischer SM, Pavone A, Mikulec C, Langenbach R, Rundhaug JE. Cyclooxygenase-2 expression is critical for chronic UV-induced murine skin carcinogenesis. Mol Carcinog. 2007; 46(5):363–71. [PubMed: 17219415]
16. Mikulec CD, Rundhaug JE, Simper MS, Lubet RA, Fischer SM. The chemopreventive efficacies of nonsteroidal anti-inflammatory drugs: the relationship of short-term biomarkers to long-term skin tumor outcome. Cancer Prev Res (Phila). 2013; 6(7):675–85. Epub 2013/05/18. DOI: 10.1158/1940-6207.CAPR-13-0064 [PubMed: 23682071]
17. Burns EM, Tober KL, Riggenbach JA, Schick JS, Lamping KN, Kusewitt DF, et al. Preventative topical diclofenac treatment differentially decreases tumor burden in male and female Skh-1 mice in a model of UVB-induced cutaneous squamous cell carcinoma. Carcinogenesis. 2013; 34(2):370–7. Epub 2012/11/06. DOI: 10.1093/carcin/bgs349 [PubMed: 23125227]
18. Torti DC, Christensen BC, Storm CA, Fortuny J, Perry AE, Zens MS, et al. Analgesic and nonsteroidal anti-inflammatory use in relation to nonmelanoma skin cancer: a population-based case-control study. J Am Acad Dermatol. 2011; 65(2):304–12. Epub 2011/05/03. DOI: 10.1016/j.jaad.2010.05.042 [PubMed: 21529996]
19. Dickinson SE, Wondrak GT. TLR4-directed Molecular Strategies Targeting Skin Photodamage and Carcinogenesis. Curr Med Chem. 2017; Epub 2017/08/30. doi: 10.2174/0929867324666170828125328

20. Weng H, Deng Y, Xie Y, Liu H, Gong F. Expression and significance of HMGB1, TLR4 and NF-kappaB p65 in human epidermal tumors. BMC Cancer. 2013; 13:311. Epub 2013/06/28. doi: 10.1186/1471-2407-13-311 [PubMed: 23803172]
21. Mittal D, Saccheri F, Venereau E, Pusterla T, Bianchi ME, Rescigno M. TLR4-mediated skin carcinogenesis is dependent on immune and radioresistant cells. EMBO J. 2010; 29(13):2242–52. Epub 2010/06/08. DOI: 10.1038/emboj.2010.94 [PubMed: 20526283]
22. Molteni M, Gemma S, Rossetti C. The Role of Toll-Like Receptor 4 in Infectious and Noninfectious Inflammation. Mediators Inflamm. 2016; 2016:6978936. Epub 2016/06/14. doi: 10.1155/2016/6978936 [PubMed: 27293318]
23. Wang X, Wang C, Wang J, Zhao S, Zhang K, Wang J, et al. Pseudoginsenoside-F11 (PF11) exerts anti-neuroinflammatory effects on LPS-activated microglial cells by inhibiting TLR4-mediated TAK1/IKK/NF-kappaB, MAPKs and Akt signaling pathways. Neuropharmacology. 2014; 79:642–56. Epub 2014/01/29. DOI: 10.1016/j.neuropharm.2014.01.022 [PubMed: 24467851]
24. Janda J, Burkett NB, Blohm-Mangone K, Huang V, Curiel-Lewandrowski C, Alberts DS, et al. Resatorvid-based Pharmacological Antagonism of Cutaneous TLR4 Blocks UV-induced NF-kappaB and AP-1 Signaling in Keratinocytes and Mouse Skin. Photochem Photobiol. 2016; 92(6): 816–25. Epub 2016/11/20. DOI: 10.1111/php.12659 [PubMed: 27859308]
25. Dickinson SE, Janda J, Criswell J, Blohm-Mangone K, Olson ER, Liu Z, et al. Inhibition of Akt Enhances the Chemopreventive Effects of Topical Rapamycin in Mouse Skin. Cancer Prev Res (Phila). 2016; 9(3):215–24. Epub 2016/01/24. DOI: 10.1158/1940-6207.CAPR-15-0419 [PubMed: 26801880]
26. Dickinson SE, Melton TF, Olson ER, Zhang J, Saboda K, Bowden GT. Inhibition of activator protein-1 by sulforaphane involves interaction with cysteine in the cFos DNA-binding domain: implications for chemoprevention of UVB-induced skin cancer. Cancer Res. 2009; 69(17):7103–10. Epub 2009/08/13. DOI: 10.1158/0008-5472.CAN-09-0770 [PubMed: 19671797]
27. Dickinson SE, Olson ER, Zhang J, Cooper SJ, Melton T, Criswell PJ, et al. p38 MAP kinase plays a functional role in UVB-induced mouse skin carcinogenesis. Mol Carcinog. 2011; 50(6):469–78. Epub 2011/01/27. DOI: 10.1002/mc.20734 [PubMed: 21268131]
28. Takashima K, Matsunaga N, Yoshimatsu M, Hazeki K, Kaisho T, Uekata M, et al. Analysis of binding site for the novel small-molecule TLR4 signal transduction inhibitor TAK-242 and its therapeutic effect on mouse sepsis model. Br J Pharmacol. 2009; 157(7):1250–62. Epub 2009/07/01. DOI: 10.1111/j.1476-5381.2009.00297.x [PubMed: 19563534]
29. Matsunaga N, Tsuchimori N, Matsumoto T, Ii M. TAK-242 (resatorvid), a small-molecule inhibitor of Toll-like receptor (TLR) 4 signaling, binds selectively to TLR4 and interferes with interactions between TLR4 and its adaptor molecules. Mol Pharmacol. 2011; 79(1):34–41. Epub 2010/10/01. DOI: 10.1124/mol.110.068064 [PubMed: 20881006]
30. Rice TW, Wheeler AP, Bernard GR, Vincent JL, Angus DC, Aikawa N, et al. A randomized, double-blind, placebo-controlled trial of TAK-242 for the treatment of severe sepsis. Crit Care Med. 2010; 38(8):1685–94. Epub 2010/06/22. DOI: 10.1097/CCM.0b013e3181e7c5c9 [PubMed: 20562702]
31. Ng SF, Rouse JJ, Sanderson FD, Meidan V, Eccleston GM. Validation of a static Franz diffusion cell system for in vitro permeation studies. AAPS PharmSciTech. 2010; 11(3):1432–41. Epub 2010/09/16. DOI: 10.1208/s12249-010-9522-9 [PubMed: 20842539]
32. Bronaugh RLaC, SW. Protocol for in vitro percutaneous absorption studies. In: Bronaugh RLaM, HI., editor. In Vitro Percutaneous Absorption: Principles, Fundamentals and Applications. Boca Raton, Florida: CRC Press; 1991. p. 237-41.
33. Franklin SJ, Dickinson SE, Karlage KL, Bowden GT, Myrdal PB. Stability of sulforaphane for topical formulation. Drug Dev Ind Pharm. 2014; 40(4):494–502. Epub 2013/04/25. DOI: 10.3109/03639045.2013.768634 [PubMed: 23611476]
34. Einspahr JG, Calvert V, Alberts DS, Curiel-Lewandrowski C, Warneke J, Krouse R, et al. Functional protein pathway activation mapping of the progression of normal skin to squamous cell carcinoma. Cancer Prev Res (Phila). 2012; 5(3):403–13. Epub 2012/03/06. DOI: 10.1158/1940-6207.CAPR-11-0427 [PubMed: 22389437]
35. Bachelor MA, Cooper SJ, Sikorski ET, Bowden GT. Inhibition of p38 mitogen-activated protein kinase and phosphatidylinositol 3-kinase decreases UVB-induced activator protein-1 and

cyclooxygenase-2 in a SKH-1 hairless mouse model. Mol Cancer Res. 2005; 3(2):90–9. Epub 2005/03/10. DOI: 10.1158/1541-7786.MCR-04-0065 [PubMed: 15755875]

36. Einspahr J, Petricoin EF, Bermudez Y, Hu C, Alberts DA, Bowden GT, Saboda K, Calvert V, Liotta L, Stratton SP. Functional Protein Pathway Activation Mapping of Normal Skin exposed to Solar Simulated Light. The Journal of Investigative Dermatology. 2013; 133(Suppl 1):S209–S21.
37. Vadlamudi RK, Joung I, Strominger JL, Shin J. p62, a phosphotyrosine-independent ligand of the SH2 domain of p56lck, belongs to a new class of ubiquitin-binding proteins. J Biol Chem. 1996; 271(34):20235–7. Epub 1996/08/23. [PubMed: 8702753]
38. Bjorkoy G, Lamark T, Johansen T. p62/SQSTM1: a missing link between protein aggregates and the autophagy machinery. Autophagy. 2006; 2(2):138–9. Epub 2006/07/29. [PubMed: 16874037]
39. Wooten MW, Geetha T, Seibenhener ML, Babu JR, Diaz-Meco MT, Moscat J. The p62 scaffold regulates nerve growth factor-induced NF-kappaB activation by influencing TRAF6 polyubiquitination. J Biol Chem. 2005; 280(42):35625–9. Epub 2005/08/05. DOI: 10.1074/jbc.C500237200 [PubMed: 16079148]
40. Gao G, Zhang T, Wang Q, Reddy K, Chen H, Yao K, et al. ADA-07 suppresses solar ultraviolet-induced skin carcinogenesis by directly inhibiting TOPK. Mol Cancer Ther. 2017; Epub 2017/06/29. doi: 10.1158/1535-7163.MCT-17-0212
41. Kuo WT, Lee TC, Yu LC. Eritoran Suppresses Colon Cancer by Altering a Functional Balance in Toll-like Receptors That Bind Lipopolysaccharide. Cancer Res. 2016; 76(16):4684–95. Epub 2016/06/23. DOI: 10.1158/0008-5472.CAN-16-0172 [PubMed: 27328732]
42. Bald T, Quast T, Landsberg J, Rogava M, Glodde N, Lopez-Ramos D, et al. Ultraviolet-radiation-induced inflammation promotes angiotropism and metastasis in melanoma. Nature. 2014; 507(7490):109–13. Epub 2014/02/28. DOI: 10.1038/nature13111 [PubMed: 24572365]
43. Chen A, Huang X, Xue Z, Cao D, Huang K, Chen J, et al. The Role of p21 in Apoptosis, Proliferation, Cell Cycle Arrest, and Antioxidant Activity in UVB-Irradiated Human HaCaT Keratinocytes. Med Sci Monit Basic Res. 2015; 21:86–95. Epub 2015/05/01. DOI: 10.12659/MSMBR.893608 [PubMed: 25925725]
44. Harberts E, Zhou H, Fishelevich R, Liu J, Gaspari AA. Ultraviolet Radiation Signaling through TLR4/MyD88 Constrains DNA Repair and Plays a Role in Cutaneous Immunosuppression. J Immunol. 2015; 194(7):3127–35. Epub 2015/02/27. DOI: 10.4049/jimmunol.1402583 [PubMed: 25716994]
45. Hou L, Bowman L, Meighan TG, Pratheeshkumar P, Shi X, Ding M. Induction of miR-21-PDCD4 signaling by UVB in JB6 cells involves ROS-mediated MAPK pathways. Exp Toxicol Pathol. 2013; 65(7–8):1145–8. Epub 2013/07/31. DOI: 10.1016/j.etp.2013.05.006 [PubMed: 23891589]
46. Lee H, Morales LD, Slaga TJ, Kim DJ. Activation of T-cell protein-tyrosine phosphatase suppresses keratinocyte survival and proliferation following UVB irradiation. J Biol Chem. 2015; 290(1):13–24. Epub 2014/11/20. DOI: 10.1074/jbc.M114.611681 [PubMed: 25406309]
47. Hanna E, Abadi R, Abbas O. Imiquimod in dermatology: an overview. Int J Dermatol. 2016; 55(8): 831–44. Epub 2016/07/09. DOI: 10.1111/ijd.13235 [PubMed: 27387373]
48. Steinhagen F, Kinjo T, Bode C, Klinman DM. TLR-based immune adjuvants. Vaccine. 2011; 29(17):3341–55. Epub 2010/08/18. DOI: 10.1016/j.vaccine.2010.08.002 [PubMed: 20713100]
49. Ran S. The Role of TLR4 in Chemotherapy-Driven Metastasis. Cancer Res. 2015; 75(12):2405–10. Epub 2015/05/23. DOI: 10.1158/0008-5472.CAN-14-3525 [PubMed: 25998620]
50. Iotzova-Weiss G, Freiberger SN, Johansen P, Kamarachev J, Guenova E, Dziunycz PJ, et al. TLR4 as a negative regulator of keratinocyte proliferation. PLoS One. 2017; 12(10):e0185668. Epub 2017/10/06. doi: 10.1371/journal.pone.0185668 [PubMed: 28982115]

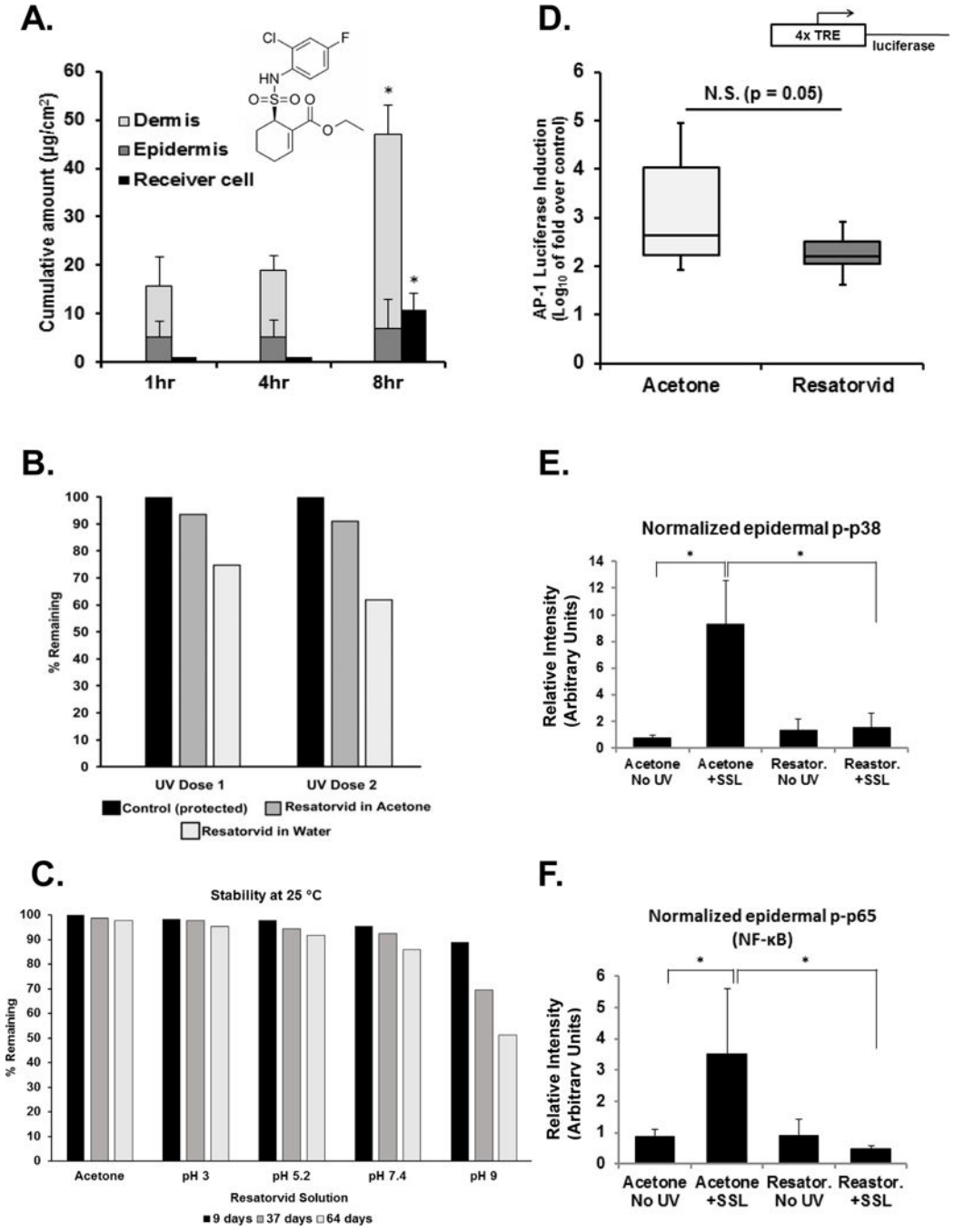

Figure 1. Topical pharmacokinetics of resatorvid enable the effective modulation of UV-induced biomarkers and AP-1 luciferase activity in mouse skin

Resatorvid (chemical structure as shown) dissolved in acetone was applied to *ex-vivo* SKH-1 mouse skin on the upper chamber of a Franz cell apparatus and transdermal penetration was quantified over time (n = 3). For quantification of total cutaneous resatorvid delivery (after removal of stratum corneum from live skin), epidermal and dermal drug contents were analyzed separately and combined.(A). The UV stability of resatorvid in acetone or water was examined in UV-permeable glass vials exposed to one or two doses of SSL (50 kJ UVA/m^2 and 2.4 kJ UVB/m^2; dose 1×), followed by quantitative HPLC (B).

Chemical stability of resatorvid in aqueous solutions of increasing pH and in acetone was examined (64 days, 25°C) (C). The ability of resatorvid to block UV-induced stress signaling *in vivo* was examined using transgenic SKH-1 AP-1 luciferase mouse models (luciferase expression under control of a 4×TPA-response element). The ears of the mice were treated with acetone (vehicle) or 10 mM resatorvid 24 hr and 1 hour prior to acute UVB. Mice were sacrificed 48 hr later and fold induction was determined by dividing the post-UV luciferase activity by the pre-UV luciferase activity of ear punches from each mouse. N.S.: not significant (D). Epidermal lysates from SKH-1 back skins post-treated with 14 mM resatorvid after acute SSL exposure were examined via western blot (p38 MAPK and p65 subunit of NFκB phosphorylation), quantified using Image J software (loading control: β-actin) (E, F). * : $p < 0.05$.

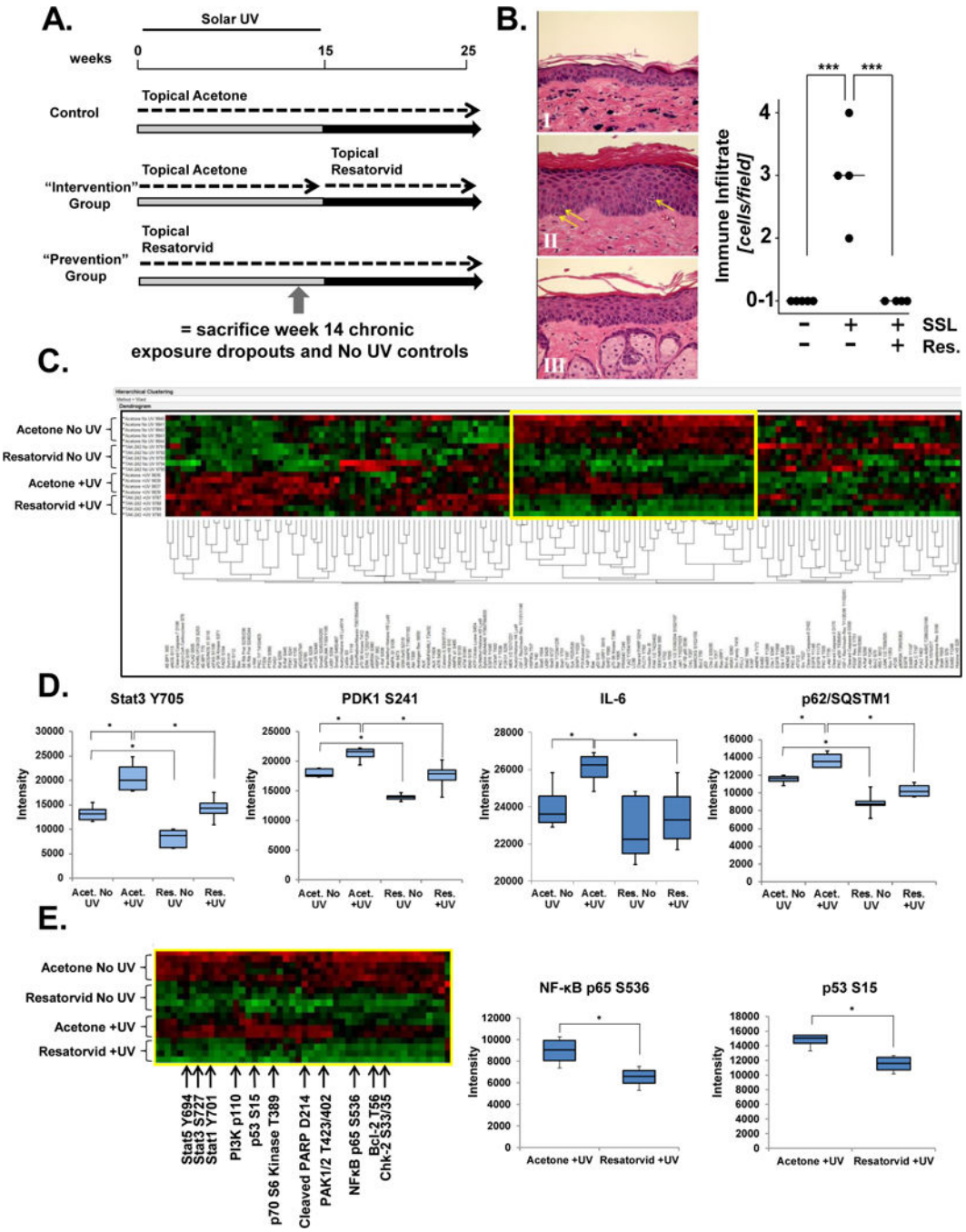

Figure 2. Resatorvid modulates UV responses in chronically exposed mouse epidermis

SKH-1 female mice were exposed to SSL three times weekly for 15 weeks, during which time they were topically treated with either vehicle (acetone) or resatorvid (10 mM, 1 hr prior to SSL). After week 15, SSL treatments stopped, but topical acetone (Control group), or resatorvid (Prevention group) continued. Another cohort (Intervention group) received topical acetone during the SSL exposures, but switched to topical resatorvid after completion of the SSL regimen until the end of the experiment (week 25). To examine the effects of UV and resatorvid in the chronic setting but before visible tumorigenesis (high-

risk skin), mice (n = 4) were sacrificed at week 14 and compared to mice treated with agent but not UV (n =5; dropout mice). The remaining mice (n = 20/group) were maintained on the protocol for the tumorigenesis study (A). Chronically exposed skin was examined for epidermal immune infiltration using H&E stained tissue (400×) (representative images, left panel). Skin was treated with vehicle (acetone) for 14 weeks (I), SSL + vehicle (II, arrows indicate lymphocytic infiltrates), or SSL + resatorvid (III). Histopathological quantification (cells/field) and morphological assignment of lymphocytic infiltrates was performed by a pathologist (right panel) (B). Epidermal lysates from the chronically-exposed dropout mice were subjected to proteomic RPPA analysis, generating an unsupervised two-way hierarchical clustering heatmap of protein/phosphoprotein expression. Each group clustered as predicted (top to bottom): Acetone No UV, Resatorvid No UV, Acetone +UV and Resatorvid +UV (C). Selected RPPA biomarkers were interrogated for resatorvid-specific inhibition of chronic UV-induced phosphorylation/expression [Stat3 (Y705), PDK1 (S241), IL-6, and p62/SQSTM1] (D). RPPA identification of a cluster of proteins (yellow box highlighted in C; partially annotated) significantly suppressed by resatorvid irrespective of chronic UV exposure, e.g. NF-κB (p65 S536) and p53 (S15) (E). * : $p < 0.05$. *** : $p < 0.001$.

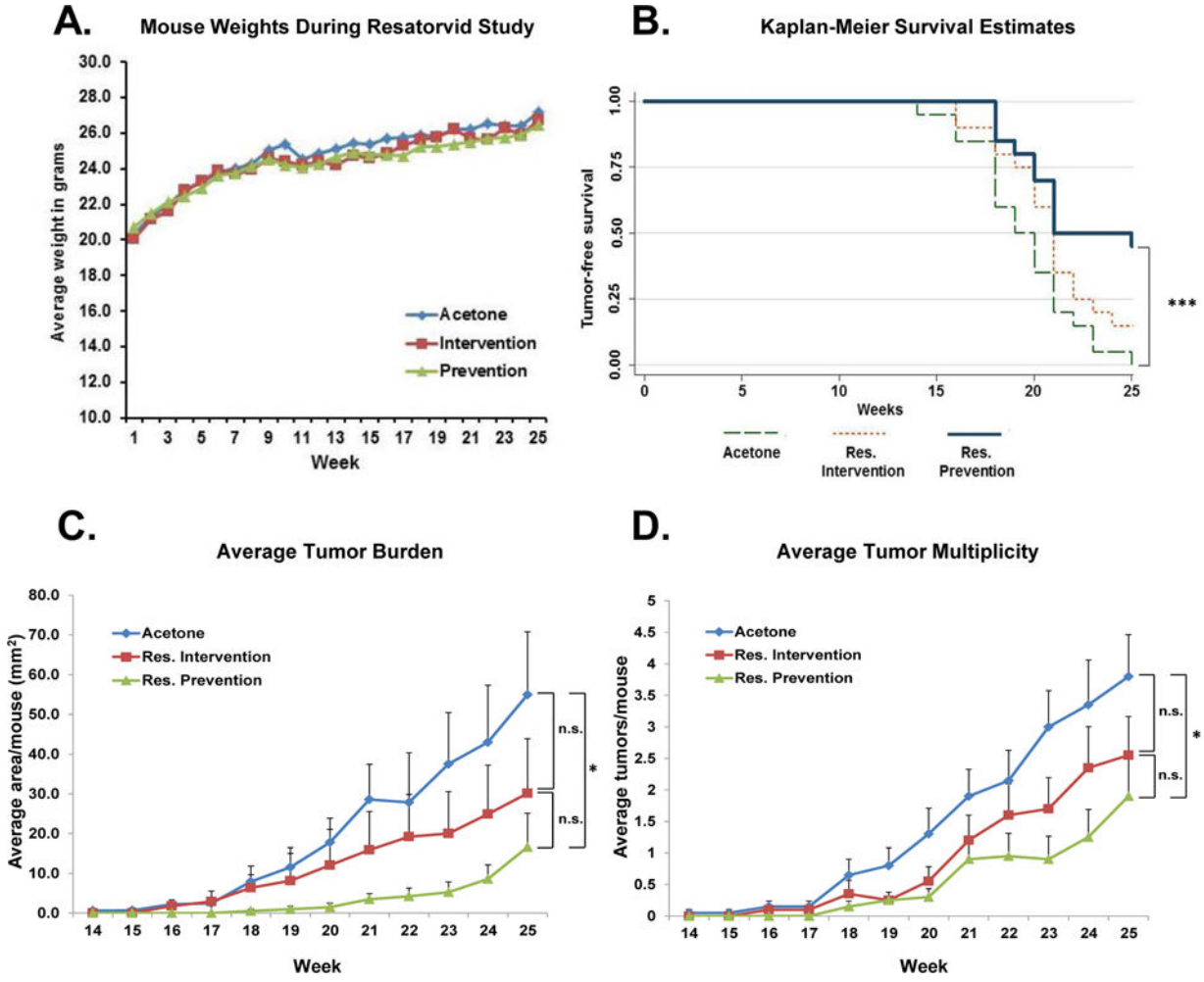

Figure 3. Topical resatorvid blocks UV-induced skin tumorigenesis in SKH-1 mice

Female SKH-1 mice were exposed to SSL three times a week for 15 weeks as described (Fig. 2A). Chronic exposure to topical resatorvid did not cause overt toxicity, as evidenced by similar weight gain between all treatment groups (A). The Resatorvid Prevention group had significantly increased tumor latency compared to acetone controls as revealed by Kaplan-Meier survival analysis (B). At sacrifice (week 25) the Resatorvid Prevention group displayed a significant reduction in average tumor burden versus the Acetone control group; the Resatorvid Intervention group displayed reduced tumor burden that was not statistically significant (C). Similarly, at sacrifice the Resatorvid Prevention group displayed significantly reduced tumor multiplicity compared to Acetone controls, while reductions in tumor multiplicity in the Resatorvid Intervention group did not reach the level of statistical significance (D). * : $p < 0.05$. *** : $p < 0.001$

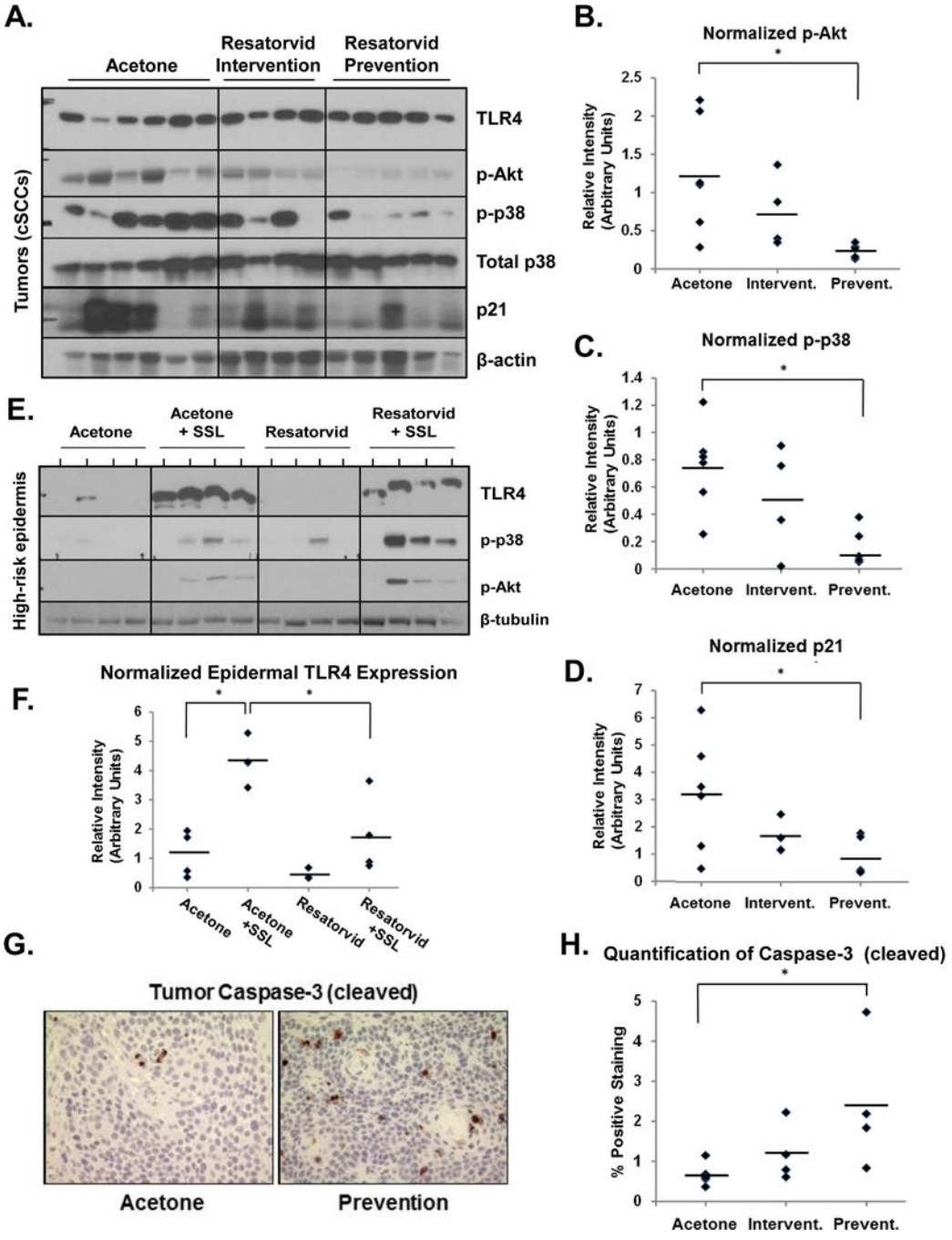

Figure 4. UV-induced tumors from resatorvid-treated mice display attenuated p38/Akt phosphorylation and increased apoptosis

Protein lysates from mouse cSCCs (Fig. 3) were subjected to Western blot analysis (A) followed by Image J-based quantification of p-Akt (normalized to total p38, B), p-p38 (normalized to total p38, C) and p21 (normalized to β-actin, D). Analogous analysis was performed using epidermal lysates from non-tumor-bearing high-risk mice (also used in Fig. 2) (E), followed by Image J-based quantification of TLR4 expression normalized against β-tubulin (F). Immunohistochemistry was performed on sections from the same tumors

described in A to probe for cleaved caspase-3 expression (400×, G), followed by quantification using ImagePro Plus software (H). * : $p < 0.05$.

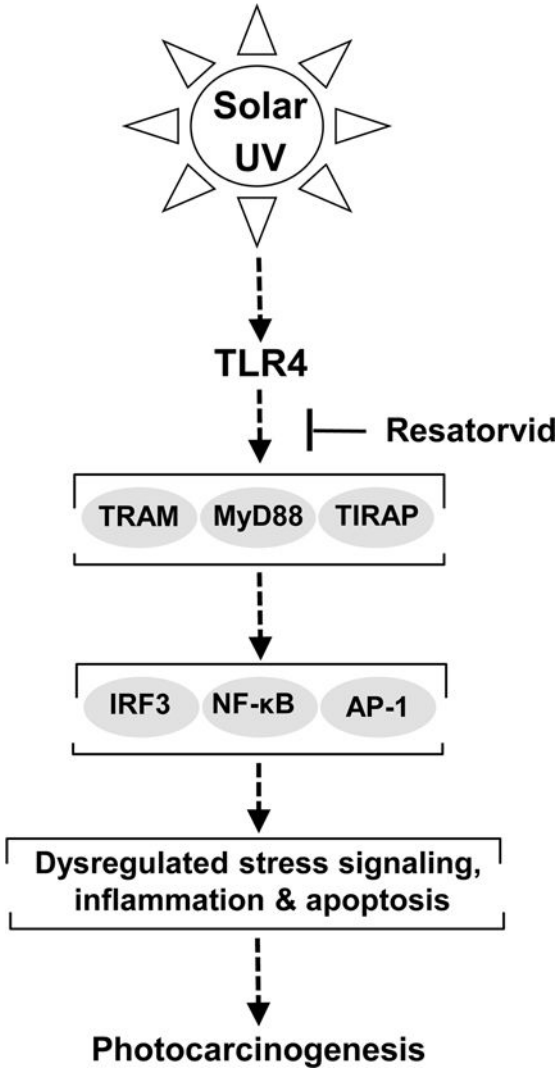

Figure 5. Resatorvid antagonizes TLR4 dependent cell signaling upstream of skin photocarcinogenesis

Resatorvid blocks TLR4 interaction with its downstream adaptor proteins containing the TIR-domain (including MyD88, TRAM/TRIF, TIRAP), thereby causing sustained suppression of multiple TLR4-dependent effector pathways, including IRF3, NF-κB and AP-1. Our findings indicate that topical pharmacological TLR4 suppression in the epidermis antagonizes chronic UV-induced inflammatory signaling and photocarcinogenesis, with potentiation of keratinocyte apoptosis.